A MIMO channel model for wireless personal area networks

Kåredal, Johan; Almers, Peter; Johansson, Anders J; Tufvesson, Fredrik; Molisch, Andreas

Published in:
IEEE Transactions on Wireless Communications

DOI:
10.1109/TWC.2010.01.090034

2010

A MIMO Channel Model for Wireless Personal Area Networks

Johan Karedal, *Member, IEEE*, Peter Almers, Anders J Johansson, *Member, IEEE*, Fredrik Tufvesson, *Senior Member, IEEE*, and Andreas F. Molisch, *Fellow, IEEE*

***Abstract*—Recent years have seen an increasing attention given to wireless Personal Area Networks (PANs), which are typically networks with small transmitter-receiver separation. The desire for high data rates has led to an interest in deploying multiple-input multiple-output (MIMO) transmission for such systems, but up until this date there exists, to the authors' best knowledge, no MIMO channel model that enables performance simulations of such systems. An important characteristic of PANs, and at the same time an important difference to regular wireless local area networks, is the interaction between the antenna array and the user. In conjunction with the irregular antenna arrangements that are typical for PAN devices, this has been shown to lead to flexible channel statistics. In this paper we present a MIMO model for PANs that incorporates these effects by prescribing different small-scale statistics and gains to different antenna elements. The proposed model can thus be seen as a generalization of the classical MIMO model for line-of-sight situations. The model is compared to several sets of measurement data and found to provide a very good description of the essential PAN channel characteristics. We also provide a detailed parameterization of the model for a particular PAN scenario.**

***Index Terms*—Personal area networks, channel measurements, MIMO, statistical channel model, irregular antenna arrays.**

I. Introduction

WIRELESS Personal Area Networks (PANs) have gained an increasing interest in recent years [1], [2]. Such networks, commonly defined as having transmitter (TX) and receiver (RX) separated by less than 10 m and located within the same room, usually involve the transmission of high data rates, and for that reason multiple-input multiple-output (MIMO) systems [3], [4], [5] seem especially suitable. This aspect was also recognized and explored in the European MAGNET project [6].

For the efficient design of any wireless system, an understanding of the propagation channel and a suitable model is necessary [7]. PAN channels differ markedly from traditional wireless local area network (WLAN) channels, which was discussed in the recent paper [8]. Three major differences were pinpointed: (i) the distance ranges are typically smaller, (ii) the antenna arrangements can be quite different with non-homogeneous element properties and (iii) an increased influence by human presence close to the antenna devices can generally be expected. These characteristics were found to produce "flexible" fast fading statistics of the channel: different antenna elements are subject to different fast fading statistics, and the fast fading statistics of an antenna element can change significantly even for small movements of the array. It was also noted that the (small-scale averaged) channel gain generally is different at different antenna elements. A model for the complete fading of the single-antenna link was presented in [8], however no MIMO modeling was considered. The current paper alleviates this gap by presenting a novel model that predicts the MIMO capabilities of PANs.

A common modeling method that automatically includes antenna correlation is to use a geometric-stochastic channel model, where scatterers are randomly placed in a geometry and their contributions summed up at the RX [9]. This approach is theoretically possible for any wireless system, but not practically feasible for PANs. This can be explained as follows. The likely reason for the flexible fading statistics observed in [8] lies in the interaction between the antenna and the user. Hence, even small movements of the user/antenna can lead to variations of the antenna patterns, such that different paths are excluded or included at different antenna elements. A geometric modeling of PAN MIMO systems with non-static TX and RX terminals thus requires knowledge of the *time-varying* antenna patterns for each individual element, which is neither easily measured nor easily implemented.

Several analytical models to include antenna correlation exist in the literature [9], e.g., the "Kronecker model" (see e.g., [10], [11]) and the models by Sayeed [12] and Weichselberger et al. [13], respectively. However, such models rely on the assumption on uniform antenna arrays, i.e., different antenna elements are assumed to follow the same fading statistics, an assumption that is not generally valid for PANs. Polarizations models [14], [15] include different mean powers (by separating co-polarized and cross-polarized power), but to the authors' best knowledge, no MIMO model that incorporates both the effects of different fading statistics and different mean power at different elements has yet been presented in the literature.

In this paper, we show that PAN MIMO channels can be modeled using a generalization of the well-known line-of-sight

Manuscript received January 9, 2009; revised June 12, 2009; accepted August 3, 2009. The associate editor coordinating the review of this paper and approving it for publication was C.-C. Chong.

J. Karedal, A. J. Johansson, and F. Tufvesson are with the Dept. of Electrical and Information Technology, Lund University, Lund, Sweden (e-mail: {Johan.Karedal, Anders.Johansson, Fredrik.Tufvesson}@eit.lth.se).

P. Almers is with ST-Ericsson, Lund, Sweden (e-mail: peter.almers@stericsson.se).

A. F. Molisch is with the Dept. of Electrical Engineering, University of Southern California, Los Angeles, CA, USA (e-mail: andreas.molisch@ieee.org).

Part of this work was funded from the SSF Center of Excellence for High-Speed Wireless Communications and a grant from the Swedish Science Council.

Digital Object Identifier 10.1109/TWC.2010.01.090034

(LOS) MIMO model of [16], i.e., by describing the channel as the sum of a dominant and a fading part. Typical characteristics of PAN systems are obtained by assigning different Ricean K–factors and different gains to the channels between different antenna elements. The proposed model does thus not claim to describe the physical reality, but rather aim at constituting a means of capturing the essential channel characteristics. By extensive comparisons to measurement data, we show that our model is able to reproduce realistic MIMO properties in terms of capacity, eigenvalue distribution and antenna correlation. We also provide a detailed parameterization of the model, applicable for a particular type of PAN scenario.

The remainder of the paper is organized as follows: Sec. II draws the outline of the model by providing a narrowband description and Sec. III verifies the modeling approach by comparisons to measurement data. Sec. IV extends the model to include temporal and frequency correlative properties whereas Sec. V provides a parameterization based on measurement data. An implementation recipe of the model is found in Sec. VI, followed by a validation of the model parameterization in Sec. VII and finally, a summary and conclusions in Sec. VIII wraps up the paper.

II. Narrowband Model

A. The LOS MIMO Model

Our modeling approach relies on the assumption that the channel can be split into a dominant and a fading part. This approach was used by Farrokhi et al. [16], who described the classical LOS MIMO channel for an $M \times N$ channel matrix $\mathbf{H}$ by[1]

$$\mathbf{H} = \sqrt{G}\left(\sqrt{\frac{K}{1+K}}\mathbf{H}^{dm} + \sqrt{\frac{1}{1+K}}\mathbf{H}^{fd}\right). \quad (1)$$

In (1), $\mathbf{H}^{dm}$ is the dominant component of the channel, available to all antenna elements and $\mathbf{H}^{fd}$ is the fading component that is randomly varying between different *antenna channels* (defined as the channel from TX array element n to RX array element m, denoted $[\mathbf{H}]_{mn}$) and whose entries are (uncorrelated) complex Gaussian with zero mean and unit variance. K is the Ricean K–factor of the system, defined as the ratio of dominant power to fading power, and G is the large-scale, local averaged, channel gain. This model thus assumes that the *only* correlating effect between the antenna channels lies in the dominant component. Furthermore, for linear antenna arrays $\mathbf{H}^{dm}$ is given by the array responses $\mathbf{a}(\theta)$ as

$$\mathbf{H}^{dm} = \mathbf{a}(\theta_r)\,\mathbf{a}(\theta_t)^T, \quad (2)$$

where θ_t and θ_r are the angle-of-departure and angle-of-arrival, respectively, and $\mathbf{a}(\theta) = \left[1\ e^{jkd\cos\theta} \ldots\ e^{jkd(L-1)\cos\theta}\right]^T$, where $k = 2\pi\lambda^{-1}$ is the wave number for a wavelength λ, for an L–element linear array with element separation d [16].

[1]Though using the notation "specular" and "scattered".

B. Proposed PAN MIMO Model

We now extend (1) by making use of two important characteristics of PAN channels [8], both due to the irregular antenna arrangements causing different antenna element to "see" different environments:

- different antenna channels can experience different small-scale statistics;
- different antenna channels can have different channel gain.

These effects are incorporated into our model by assigning *different* K–factors for the small-scale statistics[2] as well as *different* channel gains to different antenna channels. To facilitate the latter, it is suitable to split the total channel gain G of (1) into

$$G = G^{com}G^{rel}, \quad (3)$$

such that G^{com} contains the large-scale effects of distance decay and shadowing that are common to all antenna channels, whereas the gain relative G^{com} is denoted G^{rel}, which is individual for the different antenna channels. Our general model can thus be written

$$\boxed{\mathbf{H} = \sqrt{G^{com}}\mathbf{P} \odot \left(\Psi_1(\mathbf{K}) \odot \mathbf{H}^{dm} + \Psi_2(\mathbf{K}) \odot \mathbf{H}^{fd}\right),} \quad (4)$$

where

$$\mathbf{P} = \begin{bmatrix} \sqrt{G^{rel}_{11}} & \cdots & \sqrt{G^{rel}_{1N}} \\ \vdots & \ddots & \vdots \\ \sqrt{G^{rel}_{M1}} & \cdots & \sqrt{G^{rel}_{MN}} \end{bmatrix}, \quad (5)$$

$$\mathbf{K} = \begin{bmatrix} K_{11} & \cdots & K_{1N} \\ \vdots & \ddots & \vdots \\ K_{M1} & \cdots & K_{MN} \end{bmatrix}, \quad (6)$$

$\odot$ is the Schur-Hadamard product and we define the matrix functions Ψ_1 and Ψ_2 as

$$\Psi_1(\mathbf{K}) = \left[\mathbf{K} \odot [\mathbf{1}+\mathbf{K}]^{-1}\right]^{1/2}, \quad (7)$$

$$\Psi_2(\mathbf{K}) = [\mathbf{1}+\mathbf{K}]^{-1/2}, \quad (8)$$

where $[\cdot]^{1/2}$ and $[\cdot]^{-1}$ denote the element-wise square root and exponentiation with exponent -1, respectively and $\mathbf{1}$ is the $M \times N$ matrix consisting of all ones.

Since the antenna arrays of PANs are less likely to be uniformly linear, a generalized model of the dominant component in (4) also seems suitable. Ideally, we would model the phase (as well as its movement-induced variations) at the different antenna elements exactly, but as mentioned in Sec. I, this procedure requires knowledge about the antenna patterns and their sensitivity to movements. We therefore choose to neglect the phase variations[3] and instead opt for modeling the array

[2]We thus inherently use a different approach for the small-scale statistics than in [8], which modeled them as being generalized gamma distributed. Though the model of [8] indeed provides a good description of the fading of a single link, the physical interpretation of the Ricean K–factor makes the approach of this paper more appealing for MIMO modeling.

[3]Note, however, that $\mathbf{P}$ and $\mathbf{K}$ contain information about the *magnitude* of the antenna patterns variations due to movements of the arrays.

responses geometrically. Thus, we let the dominant component be given by (2), but with a slightly more general array response

$$\mathbf{a}(\theta) = \left[e^{jk\Delta_1}\ e^{jk\Delta_2} \dots\ e^{jk\Delta_L}\right]^T, \tag{9}$$

where $\Delta_i = \Delta_i(\theta)$ is the difference in geometrical path length, relative the center of the array, for array element i and an angle-of-arrival/departure θ.

A further generalization would include the correlations of the fading channels. We do not treat this here because the simpler uncorrelated model gives, as will be discussed further on, good agreement with reality.

III. Model Validation

In this section we investigate whether the proposed model of (4) can provide an adequate description of the MIMO PAN channel. We thus verify its ability to reproduce channel properties by first estimating model parameters from MIMO PAN channel measurements, using those as input to model simulations and then comparing simulated results to those obtained directly from the measurements.

A. PAN Measurements

PAN measurements were performed in an office environment using 3–element handheld devices at each end of the link, i.e., $M = N = 3$ in our evaluations.[4] The antenna arrays consist of slot antenna elements and are irregular in the sense that the elements have different orientation as well as direction (see [8], Fig. 1c). Complex channel frequency responses $H(f)$ were collected using the RUSK LUND channel sounder that performs measurements based on the switched array principle [17]. A frequency range 5.2 ± 0.1 GHz was measured, divided into $N_f = 321$ frequency points, using a test signal length of 1.6 μs.

We define large-scale movement of the terminals as movement of the TX/RX "users," whereas motion of the terminals only, i.e., while the users are standing still, is referred to as small-scale movement. Furthermore, we define *static* measurements as those where the only temporal channel variations stem from small-scale movement of the terminals, whereas *dynamic* measurements are defined as those where there is *additional* large-scale movement of the terminals *or* the environment. In the static measurements, 9 measurements with different amount of body shadowing were made for each of the 29 large-scale locations, each consisting of 10 small-scale samples of $H(f)$ recorded while slowly moving the antenna device in front of the user (thus rendering different samples with small spatial offsets). In total, 2610 static measurements were taken between various positions inside the offices, with varying shadowing inflicted on the antenna arrays and a TX-RX separation between 1 and 10 m (for details regarding the measurement setup, see [8]).

Seven different dynamic measurements were recorded, each with a duration of 10 s and a temporal increment of 18.9 ms, thus equating a total of $N_t = 500$ temporal samples. In four measurements, the users of the TX and RX devices were standing still inside an office (i.e., no large-scale movement of the terminals), while six persons were moving randomly within the same office. We distinguish between cases where people were allowed to cross the optical LOS or not, and where the users of the devices were facing each other or not. Additionally, three measurements were made while the users of the antenna devices were walking (i.e., large-scale movement of the terminals); the surroundings were static in this case.

[4]Results only make use of three out of originally four elements, since one element on the TX device was found faulty, see [8] for details.

B. Parameter Estimation

For the static measurements, the entries of $\mathbf{P}$ and $\mathbf{K}$ are estimated based on only frequency domain data, $\mathbf{H} = \mathbf{H}(f)$, i.e., 321 samples (for simplicity, the dependence on f is omitted in the subsequent equations). Maximum-likelihood estimates (MLEs) $\hat{K}_{mn}$ are derived using a grid search over $K = 0$ (linear scale) and a range from -20 to 20 dB with an increment of 0.1 dB.[5] The relative channel gain is derived as the average over frequency samples by

$$\hat{G}^{rel}_{mn} = \frac{1}{\hat{G}^{com} N_f} \sum_f \left|[\mathbf{H}]_{mn}\right|^2, \tag{10}$$

where

$$\hat{G}^{com} = \frac{1}{N_f M N} \sum_{f,m,n} \left|[\mathbf{H}]_{mn}\right|^2. \tag{11}$$

For the dynamic measurements, the statistical ensemble for estimation of K_{mn} and G^{rel}_{mn} is increased to contain frequency data collected over 5 temporal samples (i.e., a total of 321×5 samples), a time period over which the channel is considered stationary.

For each measured channel matrix, the estimated parameters $\hat{\mathbf{P}}$, $\hat{\mathbf{K}}$ and $\hat{G}^{com}$ are used with simulated matrices $\mathbf{H}^{dm}$ and $\mathbf{H}^{fd}$ in order to derive a simulated channel matrix according to (4). Since the body influence makes antenna calibration, and subsequently estimation of the angles of arrival and departure, impossible we reside to letting θ_r and θ_t be random variables in the simulation process. Furthermore, to account for a completely arbitrary orientation of the antenna arrays, we let θ_r and θ_t be uniformly distributed over $[0, 2\pi)$.[6]

C. Channel Capacity, Eigenvalue Distribution and Antenna Correlation

We derive three comparative measures from the measured as well as simulated 3×3 channel matrices: (i) the frequency-averaged channel capacity (evaluated for a signal-to-noise ratio $\rho = 20$ dB) given by

$$C = \frac{1}{N_f} \sum_f \log_2 \det\left(\mathbf{I}_M + \frac{\rho}{N}\mathbf{H}\mathbf{H}^H\right), \tag{12}$$

where $\{\cdot\}^H$ denotes the Hermitian transpose, (ii) the frequency-averaged eigenvalues of $\mathbf{H}\mathbf{H}^H$, λ_i, $i = 1, 2, 3$, and

[5]Note that there exists no closed-form expression for the MLE of K (see e.g., [18]).

[6]We thus use separate reference systems for each side of the link.

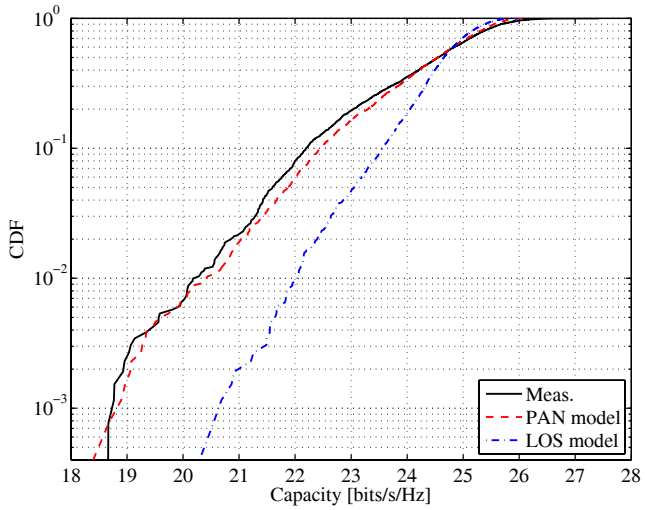

Fig. 1. CDFs of measured and simulated capacity of the static measurements.

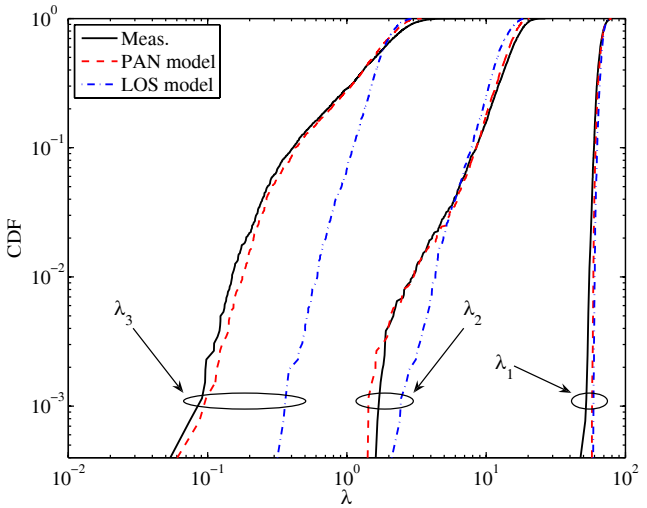

Fig. 2. CDFs of measured and simulated eigenvalues of the static measurements. The reason behind the capacity overestimation by the classical LOS model can be seen in terms of an overestimation of the weaker eigenvalues.

(iii) the frequency-averaged correlation at the TX and RX side, estimated by

$$\mathbf{R}_{TX} = \frac{1}{N_f}\sum_f \mathbf{H}^H\mathbf{H}, \tag{13}$$

$$\mathbf{R}_{RX} = \frac{1}{N_f}\sum_f \mathbf{H}\mathbf{H}^H, \tag{14}$$

respectively. In order to investigate the necessity of the higher model complexity that follows from using individual antenna channel parameters, we perform simulations using our proposed model as well as using the classical LOS model of (1) and compare the results. For the latter case, we derive $\hat{K}$ and $\hat{G}$ as the average of the individual antenna channel estimates, i.e., $\hat{K} = (MN)^{-1}\sum_{mn}\hat{K}_{mn}$ and $\hat{G} = \hat{G}^{com}(MN)^{-1}\sum_{mn}\hat{G}^{rel}_{mn}$. Furthermore, we normalize $\mathbf{H}$ such that

$$\frac{1}{N_f}\sum_f ||\mathbf{H}||_F^2 = MN, \tag{15}$$

in order to remove the influence of G^{com} in the capacity evaluations.

Fig. 1 shows cumulative distribution functions (CDFs) of the measured and simulated capacity for all static measurements, whereas Fig. 2 shows CDFs of the measured and simulated eigenvalues of $\mathbf{H}\mathbf{H}^H$. We find that the proposed model provides a very good fit to the measurement data, both in terms of predicting capacity and by correctly modeling the underlying eigenvalues. The simpler model of (1), on the other hand, greatly overestimates capacity. This can also be seen by deriving the mean squared error (MSE) between measured and simulated capacity, which is 0.5 for the proposed model whereas the classical LOS model has an MSE of 2.5.

The estimated antenna correlation suggests that the proposed model slightly underestimates capacity. Fig. 3 shows CDFs of the measured and simulated antenna correlation on the TX side (the correlation on the RX side shows similar results), and we find that the proposed model overestimates the correlation between antenna elements somewhat, an effect we subscribe to a positive bias in the K-factor estimation.

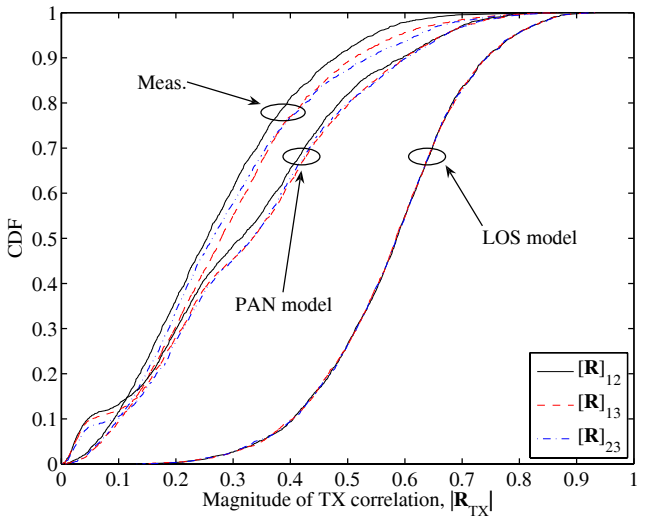

Fig. 3. CDFs of measured and simulated TX correlation of the static measurements. The proposed model overestimates the antenna correlation somewhat likely due to a bias in the K–factor estimation. The classical LOS model is not at all able of correctly describing the correlation properties.

Using only the frequency domain for estimation provides roughly 11–13 independent samples with the delay spreads we have measured, which in turn leads to an overestimation of K_{mn} (on average) that results in a higher antenna correlation. However, the overestimation of the correlation is very small, which explains why its effect is not seen in the mean absolute error between simulation and measurement (0.01).

Fig. 4 shows measured and simulated capacity for a time-varying[7] measurement: TX and RX are static, whereas a dynamic scattering environment is created by means of randomly moving people, allowed to cross the optical LOS. Again, we find that our model is well capable of describing the measured MIMO properties, which is especially encouraging since these measurements are less influenced by estimator biases due

[7]Note that even though the measurement is time-varying, model parameters are estimated at every time instant, as described in Sec. III

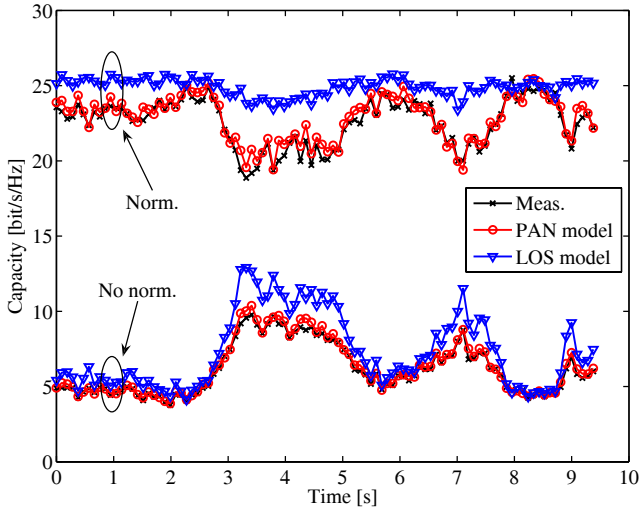

Fig. 4. Measured and simulated capacity of a time-varying measurement with no large-scale movement of the TX and RX users, whereas a small group of people are randomly moving around within the office, occasionally obstructing the optical LOS. Top curves show the capacity using normalized channels matrices according to (15), whereas the lower curves show the corresponding capacity when no normalization has been applied.

to the larger ensemble (eigenvalue distribution and TX/RX correlation are not shown for space reasons, but show a match slightly better than that of the static measurements). Similar results are obtained for all dynamic measurements. We thus conclude that the proposed model gives a good fit to all sets of measurement data and that we subsequently can model the MIMO properties of PANs accurately by properly describing the matrices $\mathbf{P}$ and $\mathbf{K}$.

IV. Extension to Time-Varying Wideband Model

Up until this point, we have seen that the proposed model works well for the narrowband case. Next, we want to extend (4) to a time-varying wideband model by inducing temporal and frequency correlation on the channel matrix, i.e., the channel frequency response matrix is given by

$$\begin{aligned}\mathbf{H}(f,t) &= \sqrt{G^{com}(t)}\mathbf{P}(t) \odot \left(\Psi_1(\mathbf{K}(t)) \odot \mathbf{H}^{dm}(f,t)\right. \\ &\quad \left. +\Psi_2(\mathbf{K}(t)) \odot \mathbf{H}^{fd}(f,t)\right). \end{aligned} \quad (16)$$

We assume that the dominant part arrives only at the first delay tap of the total channel impulse response, and rotates with a Doppler frequency f_D^{dm}. We can then compute the dominant frequency response of each antenna channel, $\left[\mathbf{H}^{dm}(f,t)\right]_{mn}$, through a Fourier transform of the corresponding one-tap dominant channel impulse response

$$\left[\mathbf{h}^{dm}(\tau,t)\right]_{mn} = e^{j\left(k(\Delta_m(\theta_r)+\Delta_n(\theta_t))+2\pi f_D^{dm}t\right)}\delta(\tau), \quad (17)$$

where $\Delta_m(\theta_r)$ and $\Delta_n(\theta_t)$ are given by (9).

The fading part of (16) can be generated using the sum-of-sinusoids method of [19]. Thus, the channel impulse response of each antenna channel of the fading part, $\left[\mathbf{h}^{fd}(\tau,t)\right]_{mn}$, is given as a sum of Q echoes, each with a phase ϕ_q, a delay τ_q and a Doppler frequency f_{D_q}, by

$$\left[\mathbf{h}^{fd}(\tau,t)\right]_{mn} = \lim_{Q\to\infty}\frac{1}{\sqrt{Q}}\sum_{q=1}^{Q} e^{j\left(\phi_q+2\pi f_{D_q}t\right)}\delta(\tau-\tau_q), \quad (18)$$

where ϕ_q, τ_q and f_{D_q} are random variables and ϕ_q is uniformly distributed over $[0, 2\pi)$. Then, the fading frequency response of each antenna channel, $\left[\mathbf{H}^{fd}(f,t)\right]_{mn}$, can be derived through a Fourier transform of (18). The modeling of f_{D_q} and τ_q is dependent on the specific scenario we attempt to model, and will hence be treated in the subsequent parameterization section.[8]

V. Model Parameterization

In this section, we address the question of parameterizing our model, since providing a parameterization is essential for the usefulness of any channel model. We thus give a description of how the model parameters vary and how they should be generated. We thus describe how to model the matrices $\mathbf{P}$ and $\mathbf{K}$, which breaks down to modeling G_{mn}^{rel} and K_{mn}, as well as the Doppler spectrum and delay dispersion of the fading components. During the latter, we also verify that the time-varying wideband model of (16) can faithfully reproduce time and frequency properties.

As noted in Sec. II, the statistical ensemble is limited in the static measurements, especially concerning the estimation of K_{mn}, which suggests that these data do not constitute a good basis for a reliable parameterization. For those reasons, the parameterization we provide in this paper is based only on the dynamic measurements we have at our disposal. However, we stress that the measurements set we base our parameterization on is still sufficiently large to give an adequate parameterization even though we may not be able to model some effects completely. Furthermore, since different fading obviously depends on different types of movement, the parameterization inevitably becomes specialized to the measured scenarios it is based upon. Here, we limit our modeling to situations with no large-scale movement of TX and RX, constant shadowing (i.e., $G^{com}(t) = G^{com}$), and a Doppler spread that is only due to the movement of scatterers (i.e., $f_D^{dm} = 0$). We do thus not make the claim that this parameterization is valid for all possible PAN scenarios, but it does serve as an *example* of parameters for a *likely* scenario; parameterization of other scenarios is left as future work.

A. Doppler Spectrum and Delay Dispersion

In theory, knowledge of the measurement geometry allows for an analytical derivation of the fading Doppler spectrum. However, such calculations are sensitive to underlying assumptions (e.g., on scatterer densities), and we therefore deem estimation of the Doppler spectrum directly from measurement data a more appealing solution. Such extractions, on the other hand, can only be done when the channel can be considered stationary, i.e., when the relative channel gain and the K-factor can be considered constant. Due to the previously discussed variations of these parameters, we therefore only use very small time intervals in our Doppler evaluations.

Fig. 5 shows an example of the measured Doppler spectrum, evaluated over 0.2 seconds of one antenna channel from a

[8]We thus model the Doppler spectrum and the fading correlation (or lack thereof) separately. While not being true in a strict sense, this approach is reasonable under our particular circumstances, i.e., given the irregular antenna arrays we are using.

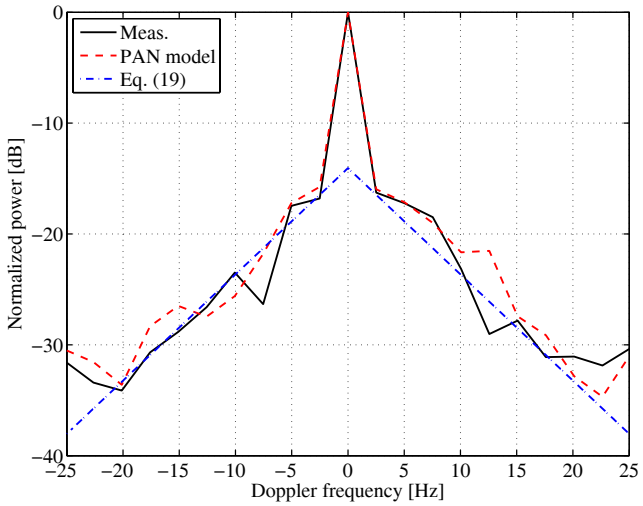

Fig. 5. Measured and simulated (using (19)) Doppler spectrum of one antenna channel from a time-varying measurement with no large-scale movement of the TX and RX users (evaluated over 0.2 seconds).

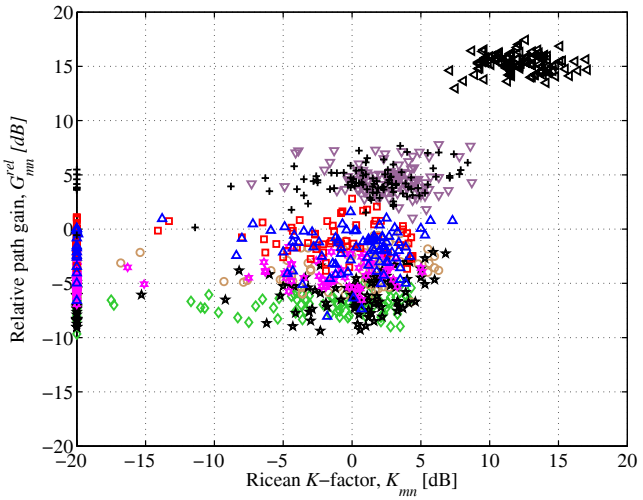

Fig. 6. $\hat{G}_{mn}^{rel}$ plotted versus $\hat{K}_{mn}$ from a time-varying measurement with no large-scale movement of the TX and RX users (dynamic scatterers are *not* allowed to cross the optical LOS). Different markers correspond to different antenna channels.

measurement with static TX and RX users. We find that the spectrum is similar in shape to those previously reported for short-range fixed systems [20], [21] which is in line with our intuition; the spectrum is centered around zero Doppler (the Doppler shift of the dominant part). Excluding the contribution at zero Doppler, we find that the *fading* part of the channel can be well described by a Laplacian Doppler spectrum

$$p\left(f_{D_q}\right) = \frac{1}{\sqrt{2}k_D} e^{-\sqrt{2}\left|f_{D_q}\right|/k_D}, \tag{19}$$

where k_D is the Doppler spread of the fading part, for the vast majority of the antenna channels. We thus let f_{D_q} in (18) be a random variable with a probability density function (PDF) $p\left(f_{D_q}\right)$, where k_D is the model parameter of interest. k_D is extracted for each 0.2 second time interval of each antenna channel of each measurement, and modeled as the ensemble mean.

The individual delays of the fading components in (18), τ_q, are modeled as exponentially distributed with a decay constant γ, following the observations in [8] that the power delay profile of the measured environment is well described by a single exponential decay. The modeling of γ is also described in [8], though we extract new parameter values from the current set of measurement data (see Table I).

In order to verify that the proposed wideband model faithfully can reproduce the temporal and frequency correlation properties of the measurements, we generate PAN MIMO channel realizations according to (16), with τ_q and f_{D_q} modeled according to the above description and $\hat{\mathbf{P}}$, $\hat{\mathbf{K}}$ and $\hat{G}^{com}$ estimated from measurement data. By studying simulated Doppler spectra (see Fig. 5 for an example) and power delay profiles we draw the conclusion that the time-variant wideband model is well capable of producing channels with the desired properties.

B. Correlation Between Parameters

The first step in parameterizing G_{mn}^{rel} and K_{mn} is to determine the correlation between them. Fig. 6 shows $\hat{G}_{mn}^{rel}$ plotted versus $\hat{K}_{mn}$ for all antenna channels of a time-varying measurement where TX and RX are static. Each marker type in the figure corresponds to a particular antenna channel and temporal samples constitute the ensembles of values. For visibility reasons, estimates $\hat{K}_{mn} = 0$ (linear scale) have been plotted at -20 dB. We find that *within* each antenna channel, $\hat{G}_{mn}^{rel}$ and $\hat{K}_{mn}$ are uncorrelated, but that there is a tendency of correlation between the *mean* values of $\hat{G}_{mn}^{rel}$ and $\hat{K}_{mn}$. However, in the measurements we have at our disposal, this result is only clearly visible in one case; the top-right ensemble of Fig. 6, which is an antenna channel that makes use of antenna elements directly aimed towards each other. Given the low occurrence rate of this observation, we choose to the neglect it and opt for modeling of not only G_{mn}^{rel} and K_{mn}, but also their means, as being uncorrelated.

Next, we analyze the parameter correlation *between* antenna channels, i.e., we derive the correlation coefficient between $\hat{K}_{mn}$ and $\hat{K}_{kl}$ for all antenna channels $[\mathbf{H}]_{mn}$ and $[\mathbf{H}]_{kl}$ except for $\{mn\} = \{kl\}$ (and similarly for $\hat{G}_{mn}^{rel}$). We find that, for both the Ricean K–factor and the relative channel gain, no correlation coefficients exceed 0.5 in magnitude, which implies that this situation can be modeled reasonably well by assuming that there is no correlation between the parameters of different antenna channels. We thus model the parameters of each antenna channel individually.

C. Relative Channel Gain

Fig. 7 shows CDFs of $\hat{G}_{mn}^{rel}$ for each antenna channel of (i) the measurement in Fig. 6, a measurement where the users of the TX and RX devices are facing each other, i.e., little body shadowing is inflicted on the antenna arrays, and (ii) a similar measurement where the users of the TX and RX devices are facing away from each other so that their bodies shadow the antenna arrays. Using χ^2-tests with 5% significance level (SL), we find that the dB-valued $\hat{G}_{mn}^{rel}$ can be well described by a Gaussian random variable. It is also notable that the mean relative channel gain can be

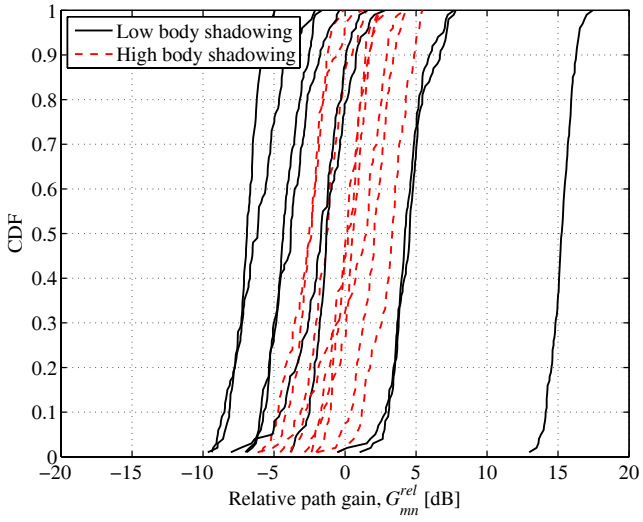

Fig. 7. CDFs of $\hat{G}^{rel}_{mn}$ for each antenna channel from two time-varying measurements with no large-scale movement of the TX and RX users, whereas dynamic scatterers are *not* allowed to cross the optical LOS. One measurement has the users of TX and RX facing each other (i.e., low body shadowing) whereas the other has the users facing away from each other (i.e., high body shadowing).

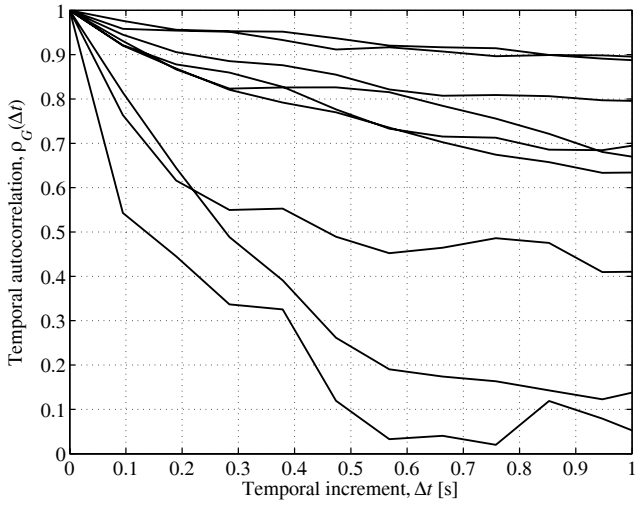

Fig. 8. Temporal autocorrelation of $\hat{G}^{rel}_{mn}$ from a time-varying measurement with no large-scale movement of the TX and RX users, dynamic scatterers not allowed to cross the optical LOS and high body shadowing level.

quite different for different antenna channels, whereas the corresponding standard deviation (STD) is fairly constant. We thus let

$$10\log_{10} G^{rel}_{mn} \sim \mathcal{N}\left(\mu^G_{mn}, \sigma_G\right), \tag{20}$$

where we model μ^G_{mn} as a Gaussian random variable (verified by another χ^2-test with 5% SL) such that

$$\mu^G_{mn} \sim \mathcal{N}\left(0, \sigma_{\mu^G}\right). \tag{21}$$

Note that the *realizations* of μ^G_{mn} should be adjusted to $\sum_{mn} \mu^G_{mn} = 0$ in order to uphold the definition of G^{rel} and G^{com}. It is furthermore interesting to note that Fig. 7 suggests that μ^G_{mn} is affected by the amount of body shadowing; the variance of μ^G_{mn} is much smaller in the case of large body shadowing than when no shadowing prevails. However, our measurement data do not allow for a complete model of this observation and we thus have to relegate the matter to future investigations.

With no large-scale movement of TX and RX and assuming a constant shadowing level, we regard G^{rel}_{mn} as a stationary stochastic process described by its autocorrelation function $\rho_G(\Delta t)$. Fig. 8 shows $\rho_G(\Delta t)$ evaluated for the "high body shadowing" measurement of Fig. 7. We find an exponential autocorrelation function

$$\rho^G_{mn}(\Delta t) = \exp\left\{-\frac{\Delta t}{k^G_{mn}} \ln 2\right\}, \tag{22}$$

where k^G_{mn} is the 50% coherence time, suitable to describe this process. Since the coherence time shows large variations between different antenna channels, it seems suitable to model it as a random variable. Showing no correlation to other model parameters, we find (using a χ^2-test with 5% SL) that k^G_{mn} can be well described by a lognormal PDF, such that

$$10\log_{10} k^G_{mn} \sim \mathcal{N}\left(\mu_{k_G}, \sigma_{k_G}\right). \tag{23}$$

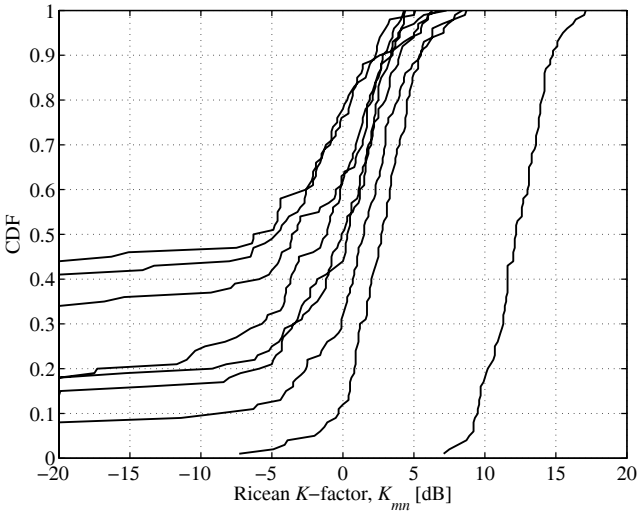

Fig. 9. CDFs of $\hat{K}_{mn}$ for each antenna channel from a time-varying measurement with no large-scale movement of the TX and RX users, whereas dynamic scatterers are *not* allowed to cross the optical LOS. Users of TX and RX are facing each other, i.e., low body shadowing is inflicted on the antenna arrays.

D. Ricean K–factor

Fig. 9 plots the CDFs of the K_{mn} estimates from Fig. 6. It is notable that the probability of an antenna channel being Rayleigh distributed ($K = 0$) is very different between antenna channels, and it seems suitable to distinguish between cases when $K = 0$ and $K \neq 0$ (linear scale).[9] We therefore model K_{mn} as a Markov process with two states, S0 ("Rayleigh state," $K = 0$) and S1 ("Ricean state," $K \neq 0$), and transition probabilities $\alpha_{mn} = \Pr\{S1|S0\}$ (the probability of shifting to S1 while in S0) and $\beta_{mn} = \Pr\{S0|S1\}$ (the probability of shifting to S0 while in S1).[10] In state S0, K_{mn}

[9]Even though there is in principle little difference between $K = 0$ and a "very low" K-factor, the large concentration at $K = 0$ makes this distinction suitable compared to using only one PDF.

[10]In the sequel, we give these probabilities relative our temporal sampling, i.e., $5 \times 18.9 = 94.7$ms

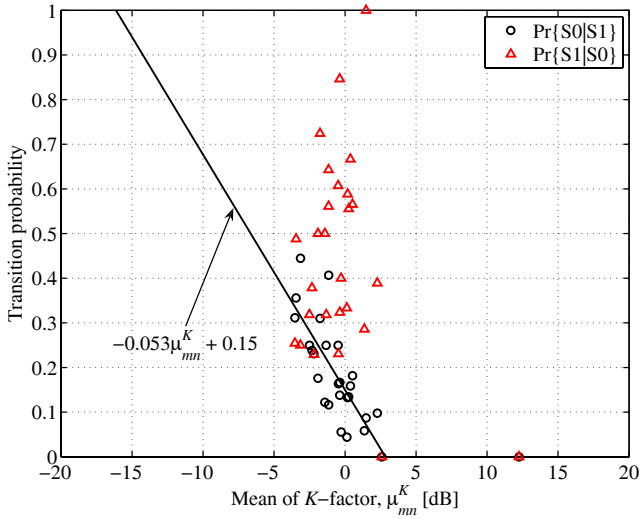

Fig. 10. The transition probabilities $\alpha_{mn} = Pr\{S1|S0\}$ and $\beta = Pr\{S0|S1\}$ plotted versus the mean of $\hat{K}_{mn}$ while in state S1.

is thus constant, whereas in state S1, we find that the dB-valued K_{mn} can be reasonably well described (using χ^2-tests with 1% SL) by a Gaussian random variable such that

$$10\log_{10} K_{mn} \sim \mathcal{N}\left(\mu^K_{mn}, \sigma_K\right), \tag{24}$$

where the standard deviation σ_K is constant since it shows only small variations between antenna channels. Similar to μ^G_{mn}, we let μ^K_{mn} be a Gaussian random variable (verified by a 5% χ^2-test), such that

$$\mu^K_{mn} \sim \mathcal{N}\left(\mu_{\mu^K}, \sigma_{\mu^K}\right). \tag{25}$$

Furthermore, we note that the transition probability β_{mn} shows a strong correlation with μ^K_{mn} (see Fig. 10), which implies that a strongly Ricean antenna channel is less prone of shifting to the Rayleigh state. We find this well described by a deterministic relationship

$$\beta_{mn}\left(\mu^K_{mn}\right) = \begin{cases} 1, & \mu^K_{mn} < -16 \\ -0.053\mu^K_{mn} + 0.15, & -16 \le \mu^K_{mn} \le 2.8 \\ 0, & \mu^K_{mn} > 2.8, \end{cases} \tag{26}$$

such that the probability of shifting to the Rayleigh state is zero if the antenna channel is "Ricean enough." The transition probability α_{mn}, on the other hand, shows no correlation with μ^K_{mn}, but is better described by a random variable. Using a χ^2-test with 5% SL, we find that a uniform distribution

$$\alpha_{mn} \sim \mathcal{U}\left(0.23, 0.72\right) \tag{27}$$

constitutes a good description.

For the same reasons mentioned in Sec. V-C, we can regard K_{mn} as a stationary stochastic process while in state S1. Here, the temporal autocorrelation of $\hat{K}_{mn}$, $\rho_K(\Delta t)$, can only be determined when $\hat{K}_{mn}$ is in the S1 state during a sufficiently long time period, which reduces the statistical ensemble somewhat. We find that also in this case, an exponential autocorrelation function

$$\rho^K_{mn}(\Delta t) = \exp\left\{-\frac{\Delta t}{k^K_{mn}}\ln 2\right\}, \tag{28}$$

is suitable, where the 50% coherence time k^K_{mn} is well described by a lognormal PDF (verified by a χ^2-test with 5% SL), such that

$$10\log_{10} k^K_{mn} \sim \mathcal{N}\left(\mu_{k^K_{mn}}, \sigma_{k^K_{mn}}\right). \tag{29}$$

VI. Implementation Recipe

Channel realizations of an $M \times N$ MIMO system can thus be generated according to our parameterized model as follows:

1) Select a suitable time window and frequency band for the simulations and select the sampling grid in time and frequency.
2) Determine the large-scale shadowing G^{com} containing distance-dependent decay, shadowing due to environment and body shadowing. Determine at the same time, for each antenna channel, the decay constant of the power delay profile γ_{mn} since this parameter is correlated with the shadowing. These parameters are described in detail in [8] and have therefore not been covered in the current paper.
3) Determine the angle-of-arrival, θ_r, and angle-of-departure, θ_t, of the dominant component from $\mathcal{U}[0, 2\pi)$.
4) Determine, for each antenna channel, the parameters of the stochastic processes $G^{rel}_{mn}(t)$: (i) the mean μ^G_{mn} from (21) and (ii) the coherence time k^G_{mn} from (23).
5) Derive, for each antenna channel, the temporal realizations of $G^{rel}_{mn}(t)$ from (20) and (22).
6) Determine, for each antenna channel, the parameters of the stochastic processes $K_{mn}(t)$: (i) the S1 mean μ^K_{mn} from (25), (ii) the S1 coherence time k^K_{mn} from (29) and (iii) the transition probabilities α_{mn} and β_{mn} from (27) and (26), respectively.
7) Derive, for each antenna channel, the temporal realizations of $K_{mn}(t)$. Start in S1 if $\alpha_{mn} > \beta_{mn}$ and in S0 otherwise. For each time instant, test if a state transition should be made. While remaining in S1, determine $K_{mn}(t)$ from (24) and (28) until the next state is S0. When changing from S0 to S1, start a new time series of $K_{mn}(t)$, i.e., disregard any correlation to previous realizations.
8) Derive the matrices $\mathbf{P}$ and $\mathbf{K}$ from (5) and (6), respectively.
9) Derive, for each antenna channel, the fading channel impulse response from (18) using γ_{mn} to derive τ_q and k_D to derive f_{D_q} from (19). A Fourier transform creates the corresponding frequency response $\left[\mathbf{H}^{fd}(f,t)\right]_{mn}$.
10) Derive, for each antenna channel, the dominant channel impulse response from (17) and derive the corresponding frequency response $\left[\mathbf{H}^{dm}(f,t)\right]_{mn}$ through a Fourier transform.
11) Derive the complete $M \times N$ time-varying channel frequency response $\mathbf{H}(f,t)$ from (16).

The model parameters σ_G, σ_{μ_G}, μ_{k_G}, σ_{k_G}, σ_K, μ_{μ_K}, μ_{μ_K}, σ_{μ_K}, μ_{k_K}, σ_{k_K}, k_D, μ_γ, and σ_γ are given in Table I.

VII. Parameterization Validation

In this section we investigate the suitability of the model parameterization in terms of its capability to reproduce MIMO

TABLE I
MODEL PARAMETERS.

Process	Description	Notation	Value	Unit
G_{mn}^{rel}	STD	σ_G	1.3	dB
	STD of mean	σ_{μ_G}	3.7	dB
	Mean of coherence time	μ_{k_G}	3.2	dBs
	STD of coherence time	σ_{k_G}	6.8	dBs
K_{mn}	STD	σ_K	4.0	dB
	Mean of mean	μ_{μ_K}	-0.2	dB
	STD of mean	σ_{μ_K}	2.6	dB
	Mean of coherence time	μ_{k_K}	3.9	dBs
	STD of coherence time	σ_{k_K}	6.3	dBs
f_{D_q}	Doppler spread (fd)	k_D	5.7	Hz
γ	Mean of decay constant (fd)	μ_γ	-79	dBs
	STD of decay constant (fd)	σ_γ	0.5	dBs

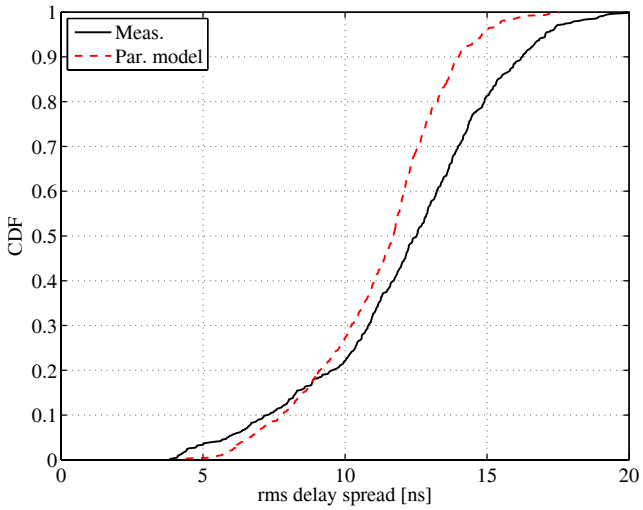

Fig. 11. The ensemble of rms delay spreads extracted from measurements, compared with that obtained from channel simulations according to the implementation recipe.

properties as well as temporal and frequency correlation. This is done by comparing simulated 3×3 MIMO channel matrices (where each channel consists of $N_f = 321$ frequency points and $N_t = 500$ temporal points) derived using the above implementation recipe to measured ones. First, we verify visually that the model produces the proper ratio between strongly fading and weakly fading channels, as well as the correct time and frequency characteristics in terms of having the desired shapes of Doppler spectra and power delay profiles. Then, in order to have a quantitative measure of the model fit, we also derive and compare: (i) the MIMO capacity according to (12), (ii) the rms delay spread and (iii) the rms Doppler spread. The latter two are derived for each measured and simulated antenna channel using 0.2 s time intervals.

The results show a mean/STD of the simulated capacity of $15.6/1.7$ bits/s/Hz (to compare with the measured values of $14.5/2.8$ bits/s/Hz), a mean/STD of the simulated rms delay spread of $11.3/2.4$ ns (measured values $12.1/3.3$ ns; see Fig. 11) and a simulated mean/STD of the rms Doppler spread of $5.0/1.3$ Hz (measured values $3.2/1.1$ Hz). We find that the difference between measured and simulated values is small, and therefore conclude that the parameterized model is well capable of representing the measured PAN scenario. The deviations between measurement and model that we do see are likely caused by the simplifying model assumptions we use, e.g., by omitting correlations between parameters. Another simplification worth mentioning is the Doppler spectrum of the fading part. Whereas the Laplacian spectrum works very well for a majority of the measured channels (as shown in Fig. 5), there are a number of channels where the spectrum has a higher weight on zero Doppler than the sum of Laplacian spectrum and the dominant part can provide (this is likely the reason behind the small overestimation of the Doppler spread). However, since we find no better suited one-parameter spectrum, and the difference in mean rms Doppler spread is small, we still deem the performance of the Laplacian spectrum satisfactory.

VIII. SUMMARY AND CONCLUSIONS

We have presented a MIMO channel model suitable for system simulations of wireless Personal Area Networks (PANs). The proposed model is a generalization of the classical LOS MIMO model which relies on the assumption that the channel can be divided into a dominant part and a fading part, the two being related by the Ricean K–factor. The key idea of our model is that we can capture the essential characteristics of PANs by prescribing *different* fading statistics (through the Ricean K–factor) and channel gain to different antenna channels (defined as the channel from TX array element n to RX array element m). In this context, we found it suitable to split the total gain of an antenna channel into one part that is common to all antenna channels, and one part, the relative channel gain, that is individual to *each* antenna channel. The proposed model was also extended to the time-varying wideband case by providing a means to include delay dispersion and Doppler spread.

A model can be validated in two senses, by answering the questions: (i) does the model description present an adequate representation of what we seek to model, i.e., is the model complexity high enough to capture the desired effects, and (ii) is the model parameterization representative to describe the measured scenarios in general? To answer the first question, we compared simulated results on capacity, eigenvalue distribution and antenna correlation to those derived from several sets of measurement data. From the good match we obtained, we concluded that our model is valid in the sense that realistic MIMO characteristics can be obtained if we can adequately describe the model parameters.

The answer to the second question is no. With our available data set, we do not claim our provided parameterization to cover *any* PAN. However, it is our opinion that the *model* is general enough to be used for other PAN scenarios, once they have been parameterized and furthermore that the detailed parameterization we provided in this paper well represents a particular PAN scenario (no large-scale movement of TX nor RX and an assumed constant shadowing level). For such situations, we found that the relative channel gain can be described as a stationary stochastic process, whose mean and coherence time varies between antenna channels and modeled the Ricean K-factor as a Markov process with two states: $K = 0$ (“Rayleigh state”) and $K \neq 0$ (“Rice state”). We

described the transition probabilities and found that while in the Rice state, K can be modeled as a stationary stochastic process, with different mean and coherence time for different antenna channels.

The paper was rounded off by an implementation recipe and thus provides everything that is needed to be used in system simulations, though the model parameterization is obviously best suited for situations similar to those covered by our measurements. Some correlative effects (e.g., the connection between relative channel gain variance and shadowing, or the correlation between the relative channel gain and the Ricean K-factor), could not be fully investigated due the limited number of measurements and are thus amongst the matters constituting a good basis for future investigations.

ACKNOWLEDGMENTS

We thank Bristol University, especially Prof. Mark Beach, for kindly lending us their antennas.

REFERENCES

[1] D. Bakker, D. M. Gilster, and R. Gilster, *Bluetooth End to End*, 1st ed. Wiley, 2002.

[2] A. Batra *et al*., "Multi-band OFDM physical layer proposal," 2003, document IEEE 802.15-03/267r2.

[3] J. H. Winters, "On the capacity of radio communications systems with diversity in Rayleigh fading environments," *IEEE J. Sel. Areas Commun.*, vol. 5, no. 5, pp. 871-878, June 1987.

[4] G. J. Foschini and M. J. Gans, "On limits of wireless communications in a fading environment when using multiple antennas," *Wireless Personal Commun.*, vol. 6, pp. 311-335, Feb. 1998.

[5] A. Paulraj, D. Gore, and R. Nabar, *Multiple Antenna Systems*. Cambridge, U.K.: Cambridge University Press, 2003.

[6] [Online]. Available: http://web.archive.org/web/20071024180734/http://www.ist-magnet.org/.

[7] A. F. Molisch, *Wireless Communications*. Chichester, West Sussex, UK: IEEE Press–Wiley, 2005.

[8] J. Karedal, A. J. Johansson, F. Tufvesson, and A. F. Molisch, "A measurement-based fading model for wireless personal area networks," *IEEE Trans. Wireless Commun.*, vol. 7, no. 11, pp. 4575-4585, Nov. 2008.

[9] P. Almers, E. Bonek, A. Burr, N. Czink, M. Debbah, V. Degli-Esposti, H. Hofstetter, P. Kyoesti, D. Laurenson, G. Matz, A. Molisch, C. Oestges, and H. Oezcelik, "Survey of channel and radio propagation models for wireless MIMO systems," *EURASIP J. Wireless Commun. Networking*, vol. 2007.

[10] J. P. Kermoal, L. Schumacher, K. I. Pedersen, P. E. Mogensen, and F. Frederiksen, "A stochastic MIMO radio channel model with experimental validation," *IEEE J. Sel. Areas Commun.*, vol. 20, no. 6, pp. 1211-1226, Aug. 2002.

[11] D. P. McNamara, M. A. Beach, and P. N. Fletcher, "Spatial correlation in indoor MIMO channels," in *Proc. IEEE Int. Symp. Personal, Indoor, Mobile Radio Commun.*, vol. 1, Lisbon, Portugal, 2002, pp. 290-294.

[12] A. M. Sayeed, "Deconstructing multiantenna fading channels," *IEEE Trans. Signal Process.*, vol. 50, no. 10, pp. 2563-2579, Oct. 2002.

[13] W. Weichselberger, M. Herdin, H. Özcelik, and E. Bonek, "A stochastic MIMO channel model with joint correlation of both link ends," *IEEE Trans. Wireless Commun.*, vol. 5, no. 1, pp. 90-100, Jan. 2006.

[14] M. Shafi, M. Zhang, A. L. Moustakas, P. J. Smith, A. F. Molisch, F. Tufvesson, and S. H. Simon, "Polarized MIMO channels in 3-D: models, measurements and mutual information," *IEEE J. Sel. Areas Commun.*, vol. 24, no. 3, pp. 514-527, Mar. 2006.

[15] M. Coldrey, "Modeling and capacity of polarized MIMO channels," in *Proc. IEEE Veh. Technol. Conf. 2008 Spring*, Singapore, May 2008, pp. 440-444.

[16] F. Rashid-Farrokhi, A. Lozano, G. Foschini, and R. Valenzuela, "Spectral efficiency of wireless systems with multiple transmit and receive antennas," in *Proc. IEEE Int. Symp. Personal, Indoor, Mobile Radio Commun.*, vol. 1, Sep. 2000, pp. 373-377.

[17] R. Thomae, D. Hampicke, A. Richter, G. Sommerkorn, A. Schneider, U. Trautwein, and W. Wirnitzer, "Identification of the time-variant directional mobile radio channels," *IEEE Trans. Instrum. Meas.*, vol. 49, no. 2, pp. 357-364, Sep. 2000.

[18] C. Tepedelenlioglu, A. Abdi, and G. B. Giannakis, "The Ricean K factor: estimation and performance analysis," *IEEE Trans. Wireless Commun.*, vol. 2, no. 4, pp. 799-810, July 2003.

[19] P. Hoeher, "A statistical discrete-time model for the WSSUS multipath channel," *IEEE Trans. Veh. Technol.*, vol. 41, no. 4, pp. 461-468, Nov. 1992.

[20] A. Domazetovic, L. J. Greenstein, N. B. Mandayam, and I. Seskar, "Estimating the Doppler spectrum of a short-range fixed wireless channel," *IEEE Commun. Lett.*, vol. 7, no. 5, pp. 227-229, May 2003.

[21] P. Pagani and P. Pajusco, "Characterization and modeling of temporal variations on an ultrawideband radio link," *IEEE Trans. Antennas Propag.*, vol. 54, no. 11, pp. 3198-3206, Nov. 2006.

Johan Karedal received his M.S. degree in engineering physics in 2002 and his Ph.D. in radio communications in 2009, both from Lund University, Sweden. He is currently a postdoctoral fellow at the Department of Electrical and Information Technology, Lund University, where his main research interests concern measurements and modeling of the wireless propagation channel for MIMO and UWB systems. Dr. Karedal has participated in the European research initiative "MAGNET."

Peter Almers received the M.S. degree in electrical engineering in 1998 and his Ph.D. degree in 2007, both from Lund University, Sweden. Currently he is a senior staff engineer at ST-Ericsson, Lund, Sweden. Between 1998 and 2006, he was also with the radio research department at TeliaSonera AB (formerly Telia AB), in Malmö, Sweden, mainly working with WCDMA and 3GPP standardization physical layer issues. From 2007 to 2008, he worked as a research fellow at the Department of Electrical and Information Technology, Lund University.

Dr. Almers has participated in the European research initiatives "COST273," the European network of excellence "NEWCOM" and the NORDITE project "WILATI." He received an IEEE Best Student Paper Award at PIMRC in 2002.

Anders J Johansson received his M.S., Lic. Eng. and Ph.D. degrees in electrical engineering from Lund University, Lund, Sweden, in 1993, 2000 and 2004 respectively. From 1994 to 1997 he was with Ericsson Mobile Communications AB developing transceivers and antennas for mobile phones. Since 2005 he is an Associate Professor at the Department of Electrical and Information Technology, Lund University. His research interests include antennas, wave propagation and telemetric devices for medical implants as well as antenna systems and propagation modelling for MIMO systems.

Fredrik Tufvesson was born in Lund, Sweden in 1970. He received the M.S. degree in electrical engineering in 1994, the Licentiate Degree in 1998 and his Ph.D. in 2000, all from Lund University in Sweden. After almost two years at a startup company, Fiberless Society, Fredrik is now associate professor at the Department of Electrical and Information Technology. His main research interests are channel measurements and modeling for wireless communication, including channels for both MIMO and UWB systems. Beside this, he also works with channel estimation and synchronization problems, OFDM system design and UWB transceiver design.

Andreas F. Molisch received the Dipl. Ing., Dr. techn., and habilitation degrees from the Technical University Vienna (Austria) in 1990, 1994, and 1999, respectively. From 1991 to 2000, he was with the TU Vienna, becoming an associate professor there in 1999. From 2000 to 2002, he was with the Wireless Systems Research Department at AT&T (Bell) Laboratories Research in Middletown, NJ. From 2002 to 2008, he was with Mitsubishi Electric Research Labs, Cambridge, MA, USA, most recently as Distinguished Member of Technical Staff and Chief Wireless Standards Architect. Concurrently he was also Professor and Chairholder for radio systems at Lund University, Sweden. Since 2009, he is Professor of Electrical Engineering and Head of the Wireless Devices and Systems (WiDeS) group at the University of Southern California, Los Angeles, CA, USA.

Dr. Molisch has done research in the areas of SAW filters, radiative transfer in atomic vapors, atomic line filters, smart antennas, and wideband systems. His current research interests are measurement and modeling of mobile radio channels, UWB, cooperative communications, and MIMO systems. Dr. Molisch has authored, co-authored or edited four books (among them the textbook *Wireless Communications*, Wiley-IEEE Press); 11 book chapters, more than 120 journal papers, and numerous conference contributions, as well as more than 70 patents and 60 standards contributions.

Dr. Molisch is Area Editor for Antennas and Propagation of the IEEE TRANSACTIONS ON WIRELESS COMMUNICATIONS and co-editor of special issues of several journals. He has been member of numerous TPCs, vice chair of the TPC of VTC 2005 spring, general chair of ICUWB 2006, TPC co-chair of the wireless symposium of Globecomm 2007, TPC chair of Chinacom2007, and general chair of Chinacom 2008. He has participated in the European research initiatives "COST 231," "COST 259," and "COST273," where he was chairman of the MIMO channel working group, he was chairman of the IEEE 802.15.4a channel model standardization group. From 2005 to 2008, he was also chairman of Commission C (signals and systems) of URSI (International Union of Radio Scientists), and since 2009, he is the Chair of the Radio Communications Committee of the IEEE Communications Society. Dr. Molisch is a Fellow of the IEEE, a Fellow of the IET, an IEEE Distinguished Lecturer, and recipient of several awards.